

SUPPLEMENTAL MATERIAL

Supplemental Methods

1. Generation of fate-mapping transgenic mice.

Transgenic β -actin-GFP mice and fate-mapping double transgenic mice (Myh6-MerCreMer-lacZ or Myh6-MerCreMer-tdTomato) were used in our study. They were generated by crossbreeding B6.FVB(129)-Tg(Myh6-cre/Esr1*)1Jmk/J mice with B6.129S4-Gt(ROSA) 26Sortm1Sor/J mice or B6.Cg-Gt(ROSA)26Sortm14(CAG-tdTomato)Hze/J (Jackson Laboratory).

The Myh6-MerCreMer-lacZ (or -tdTomato) mice have the mouse cardiac-specific alpha-myosin heavy chain promoter directing expression of a tamoxifen-inducible Cre recombinase (MerCreMer) in juvenile and adult cardiomyocytes. As described previously,¹ Cre recombination and lacZ (or tdTomato) labelling in cardiomyocytes were induced by 4-OH-tamoxifen pulse injection. Four-month-old fate-mapping mice were intraperitoneally injected with 4-OH-tamoxifen (Sigma, Cat. No. H-6278) dissolved in peanut oil (Sigma, Cat. No. S5007) at a concentration of 5 mg/ml at a dosage of 20 mg/kg per day for 7 days. Seven days after the last injection of 4-OH-tamoxifen, fate-mapping mice were ready for use.

Animal care and all experimental procedures were performed in strict accordance with the approved protocols and animal welfare regulations of the Animal Care and Use Committee at Third Military Medical University. All surgery was performed under isoflurane anesthesia, and all efforts were made to minimize suffering.

2. Isolation and culture of adult cardiomyocytes (ACMs), neonatal rat ventricular myocytes (NRVMs), fetal mouse cardiomyocytes (FCMs) and cardiac fibroblasts.

2.1 ACMs: ACMs were isolated and cultured according to the methods described previously.²

2.2 NRVMs and cardiac fibroblasts: NRVMs were isolated from 1-2-day-old Sprague-Dawley rat pups using the method described previously in detail.³ Briefly, the hearts were removed from the pups immediately after euthanasia, the ventricles were minced, and the cardiomyocytes were dissociated with trypsin (1.5 mg/mL, GIBCO). These cells were then re-suspended in DMEM (GIBCO) supplemented with 10% FBS (Hyclone) and 0.1 mM BrdU, and plated in culture dishes for 60 minutes to allow fast-adherent cells to attach. Non-adherent cells (cardiomyocytes) were collected and plated in different culture dishes or coverslips coated with fibronectin at a density of 150 cells per mm². On the following day, the medium was replaced with 10% FBS-DMEM but without BrdU.

Neonatal rat cardiac fibroblasts were isolated as previously described.⁴ Fast-adherent cells (non-cardiomyocytes, mostly fibroblasts) were cultured in 10% FBS-DMEM and allowed to grow to confluence. Cells at third passage were used for experiments.

2.3 FCMs: Similar to the method described previously,⁵ day 15 embryonic hearts were digested with

1 collagenase I for 60 minutes at 37°C. Dissociated FCMs were plated on fibronectin-coated dishes at a
2 density of 150 cells per mm², and cultured in DMEM supplemented with 10% FBS and antibiotics.

3 4 **3. Mouse ACM viability in culture**

5 Trypan blue staining was applied to determine cardiomyocyte survival. Cells were stained for 10 minutes
6 at room temperature at a final concentration of 0.04% (wt/vol). Cells taking up trypan blue were stained
7 blue and considered dead.⁶ For ACMs isolated from transgenic β -actin-GFP mice, GFP positive/trypan
8 blue negative cells were counted as live cells.

9 10 **4. Co-culture of ACMs with feeding layers and quantification of the spontaneous contraction**

11 For mixed co-culture study, GFP⁺ ACMs were seeded on top of a feeding layer of NRVMs, FCMs or
12 fibroblasts. The ACMs and the feeder cell types were plated at a ratio of 1:20 and cultured for up to 7
13 days. Other ratios, such as 1:5, 1:10, 1:50, and 1:100, were tested in initial experiments to optimize the
14 protocol. For controls, cultured GFP⁺ ACMs were maintained in regular medium or conditioned medium
15 of NRVMs.

16 To quantify the spontaneous contractions of the GFP⁺ ACMs, the co-cultures were trypsinized and
17 placed into a new dish to form a monolayer with lower density (without cell-cell connections). The
18 spontaneously contracting GFP⁺ ACMs were counted under an inverted fluorescence microscope (Nikon,
19 Japan) by in blinded manner. Since the co-cultured cells become confluent after 7 days culture, this
20 method can discriminate between the contractile activity of GFP-positive cells and co-cultured NRVMs
21 or FCMs.

22 23 **5. Time-lapse imaging microscopy**

24 To capture cell division events in ACMs *in-vitro*, we carried out a long-term time-lapse microscopy using
25 an Olympus IX83 inverted microscope with a humidified cell culture chamber in the presence of 5% CO₂
26 at 37°C. ACMs isolated from β -actin-GFP transgenic mice or Myh6-MerCreMer-tdTomato fate-mapping
27 mice were expressing GFP fluorescence. Before co-culture with NRVMs, ACMs were pretreated with
28 Thermo Scientific DRAQ5™ Fluorescent Probe (5 mM for 10 minutes) to label the nuclei with infrared
29 fluorescence. Once upon coculture, 100 random fields of 10 \times objective lens were selected and the
30 positions were marked with the “position-list” tool in the microscopy software. The time-lapse images
31 were taken at intervals of one hour for 7 days. Time-lapse movies were generated after the end of each
32 experiment and exported as .AVI files.

33 34 **6. Development of Cx43 mutants and cell transduction in hypoxia**

35 Mouse Cx43 mutant with serines 325/328/330 replaced by phosphomimetic glutamic acids (S3E)
36 or by nonphosphorylatable alanines (S3A) were gifted by Dr. Glenn I. Fishman at New York University

1 School of Medicine.⁷ Cx43-S3E were resistant to pathological gap junction remodeling induced by
2 cardiac ischemia.⁷

3 In the ACM and NRVM co-culture system, cells were transduced with vector, cx43 wild type
4 (WT), Cx43-S3A or Cx43-S3E over-expression plasmids. The transduction was performed with
5 lipofectamine 2000 (Invitrogen, cat#11668) according to the manufacture's instruction. Twenty-four
6 hours after plasmids transduction, cells were placed in a hypoxic condition to induce Cx43
7 dephosphorylation as previously described.⁸ Hypoxia was induced in an environmental chamber
8 containing 5% O₂, 5% CO₂ (balance N₂) for 72 hours.

9 10 **7. Production of adeno-associated virus 9 (AAV9)-Cx43 mutant and its delivery post mouse** 11 **myocardial infarction (MI)**

12 Recombined AAV9-Cx43-S3E is produced in human 293T cells with insertion of Cx43-S3E
13 mutant sequence into AAV9 vector. Cx43 cDNA was firstly amplified with primers (P1:
14 aacccccggtccggtagcgcgccaccatgggtgactggagcgccttgg; P2: caccatgccagatccgccgatccaatctccaggta tcaggccga)
15 and fused into pAOV-CAG-EGFP vector (Neuronbiotech, Shanghai, China) with seamless-cloning
16 method and sequenced. Then the engineered vector was co-transfected with pHelper and pRC (for AAV9
17 rep and cap expression) plasmid to 293T cells for viral production. After 72h incubation, cells were
18 harvested and disrupted. rAAV9 particles were isolated with freeze-thaw method and purified by CsCl
19 concentration gradient centrifugation for 48h, with two rounds. Virus was titered with qPCR test to WPRE
20 sequence and stocked at -80 °C. AAV9 for with scramble sequence were used as control in the
21 experiments.

22 Mouse MI model were performed according to the methods we described previously.⁹ Under
23 anesthesia with isoflurane inhalation, permanent ligation of left anterior descending (LAD) coronary
24 artery was performed. Sham-operated mice were subjected to the same surgical procedures except tying
25 the suture. Three days after after MI injury, AAV9-Cx43-S3E or AAV9-scramble was intravenously
26 injected via the tail vein. Each animal was injected with 125 μL viral solution containing 5×10¹⁰ viral
27 particles, similar to previous studies.¹⁰

28 29 **8. Histology and immunostaining**

30 For immunocytochemistry, cells were fixed with paraformaldehyde for immunostaining. For tissue
31 section histopathology, paraffin embeded sections of mouse heart tissues were used.

32 Cells or tissue sections were incubated with primary antibody overnight at 4°C. The following
33 primary antibodies were used: sarcomeric tropomyosin (Sigma, cat#T9283), troponin I (Santa Cruz,
34 cat#sc-15368), Runx1 (Epitomics, cat#2593-1), Dab2 (BD biosciences, cat#610465), nuclear factor of
35 activated T cells c3 (NFATc3) (Santa Cruz, cat#sc-8375), Ki67 (Abcam, cat#ab15580) and
36 Phosphohistone H3 (PH3) (Millipore, cat#06-570). Alexa fluor[®] 555 Donkey anti-rabbit IgG(H+L)

1 (Molecular Probes[®], Life technologies, cat#A-31572)、Alexa fluor[®] 488 Donkey anti-mouse IgG (H+L)
2 (Molecular Probes[®], Life technologies, cat#A-21202), or Alexa fluor[®] 647 Donkey anti-goat IgG (H+L)
3 (Molecular Probes[®], Life technologies, cat#A-21447), Dylight 405 Donkey anti-mouse IgG (H+L)
4 (Jackson ImmunoResearch, cat#714-475-151) were applied appropriately. Nuclei were labeled with DAPI
5 (Sigma, cat#D9542). Negative control cells were performed under the same conditions but without
6 primary antibodies. The organized sarcomere is identified by the clear striation myofibril pattern detected
7 with cTnI staining or tropomyosin.¹¹

8 For EdU incorporation analysis in AAV9-S3E treated mice, EdU was administered
9 intraperitoneally (500 µg per animal) every 2 days after AAV9-S3E administration, for a period of ten
10 days (5 shots) as previously described.¹² The hearts were then harvested and isolated into individual
11 ACMs. These isolated ACMs were then staining with EdU antibody and quantified. The procedures were
12 performed by using a commercially available kit (Invitrogen) per the manufacturer's instructions.

13 Images were taken at with a Nikon fluorescence microscope (Tokyo, Japan) and Olympus confocal
14 microscope (FluoView 1000, Japan). All the manual counts were performed in a blinded fashion.
15

16 **9. Lineage tracing of pre-existing ACMs with β-galactosidase (β-gal) staining**

17 The lacZ staining of heart tissue or isolated ACMs in Myh6-MerCreMer-lacZ mice was carried out
18 as described previously with minor modification.^{1, 13} For lacZ staining on heart tissue, the lacZ detection
19 kit for tissues was used (Invivogene, cat#rep-lz-t). Heart tissue was dissect in PBS/MgCl₂ (2mmol/L) on
20 ice, then fixed in 2.5% Glutaraldehyde on ice for 30min. After rinsed several times in PBS, the tissue was
21 incubated in freshly prepared staining solution (6mM Potassium Ferricyanide, 6mM Potassium
22 Ferrocyanide, 2mM Mgcl₂, 0.02% Igepal, 0.01% Na deoxycholate, 10mg/ml X-Gal (5-bromo-4-chloro-3-
23 indoyl-β-D-Galactopyranoside), 0.01M PBS) at 37°C overnight. After 5 times wash in PBS, the
24 development of blue color was checked under a microscope. For lacZ staining on isolated cardiomyocytes,
25 the lacZ detection kit for cells (Invivogene, cat#rep-lz-c) was used. Cells were washed three times with
26 PBS and fixed in Fix solution at room temperature for 10mins. After washed three times with PBS, cells
27 were incubated in freshly prepared staining solution (4mM Potassium Ferricyanide, 4mM Potassium
28 Ferrocyanide, 2mM Mgcl₂, 0.84 mg/ml X-Gal, 0.01M PBS) for six hours. The development of blue color
29 was checked under a microscope.

30 For detection of lacZ by immunofluorescence staining, tissue or cells were fixed and prepared
31 following standard histological procedure, similar to previously described.¹⁴ Both paraffin embedded
32 section and cyro-section were used. To investigate other protein or markers in pre-existing
33 cardiomyocytes, multiple antibodies including anti-lacZ antibody (Santa Cruz, cat#sc-19119) were
34 incubated with samples and visualized by secondary antibodies in a certain order.
35

36 **10. Infarct size determination**

1 Similar to previously described,¹⁵ hearts (4 weeks post-MI) were fixed in 4% paraformaldehyde in
2 PBS processed, embedded in paraffin and cut as 5 μm -thick sections. Masson's trichrome staining was
3 performed according to standard procedures. The percentage of fibrotic area of left ventricle was
4 measured using Image J software, and the values obtained were averaged. Individuals conducting the
5 experiment were blinded to the experimental groups.

7 **11. Echocardiography analysis**

8 Echocardiography was performed (GE vivid 9 dimension) following the methods we described
9 previously.⁹ Briefly, hearts were viewed in the short-axis with M-mode by averaging results from three
10 consecutive heart beats. LVIDd (diastolic left ventricle internal diameter) and LVIDs (systolic left
11 ventricle internal diameter.) were measured to determine structural changes in cardiac morphology.
12 Fractional shortening (%FS) was calculated as $(\text{LVIDd} - \text{LVIDs})/\text{LVIDd} \times 100$. Left ventricle ejection
13 fraction (EF%) was automatically calculated according to the Teicholz formula. The individuals
14 conducting the experiment were blinded to the animal treatments.

16 **12. Measurement of calcium transients**

17 Calcium transients of NRVMs were measured using a protocol similar to our previous studies.² In
18 brief, NRVMs on coverslips were placed in a heated chamber (25°C) on a stage of an inverted
19 microscope (Nikon Eclipse 200) with a Ionopix Myocyte Calcium and Contractility System. NRVMs
20 loaded with a fluorescent Ca^{2+} indicator, indo-1 AM, were perfused with a Tyrode solution containing 1
21 mM CaCl_2 and Ca^{2+} transients (intracellular Ca^{2+} concentration, $[\text{Ca}^{2+}]_i$) were measured at the pacing
22 frequency of 0.5 Hz.

24 **13. Fluorescence recovery after photobleaching (FRAP) analysis**

25 To directly measure reduced cell-cell coupling, we measured fluorescence recovery after
26 photobleaching (FRAP) and showed that Cx43-siRNA reduced gap junction communication between
27 ACMs and NRVMs. 5×10^4 NRVMs per 35mm cell culture surface (Corning) were loaded with dye by
28 incubation for 15 min with 4 $\mu\text{mol/L}$ calcein red-orange AM (Invitrogen) in Hank's balanced salt solution
29 (Invitrogen). Thereafter, the cells were rinsed three times with PBS and were kept in the incubator in
30 medium supplemented with 2.5mmol/L probenecid (Invitrogen) for ≥ 30 min before 2.5×10^3 ACMs were
31 added.

32 Freshly isolated ACMs (GFP-positive) were maintained in DMEM with 10% FBS medium added
33 with 20mM BDM (Diacetyl monoxime, TCI, cat#B0683). ACMs were pretreated with mouse specific
34 Cx43-siRNA or scramble-siRNA 24 hours before co-culture with NRVMs. A scramble-siRNA labeled
35 with Cy3 fluorescence was also used to monitor the transfection efficiency.

36 FRAP assay were performed after pretreated ACMs (GFP-positive) were co-cultured onto NRVMs.

1 ACMs attached to neighboring NRVMs were located using a Leica TCS SP5 confocal microscopy.
2 Intracellular calcein in the ACMs was photo-bleached using a 550nm excitation light for 3 frames. ACMs
3 were then allowed to recover from the photo-bleach for 200 seconds. The intracellular calcein recovery
4 was recorded with specified interval.

6 **14. Drug and siRNA administration**

7 To explore the role of Ca^{2+} regulation in ACM dedifferentiation/redifferentiation, a SERCA
8 inhibitor (thapsigargin, 0.1 μ M) and an intracellular Ca^{2+} chelator, 1,2-bis(2-aminophenoxy)ethane -
9 *N,N,N',N'*-tetraacetic acid tetrakis (acetoxymethyl) ester (BAPTA-AM, 1 μ M) were used.

10 Mouse specific siRNA of Cx43, calcineurin, NFATC3 and MEF2C were used to block the related
11 gene expressions. The siRNA sequences were as follow: mouse Cx43: 5'
12 TAGAAGATTCAAAGAGCTTAA 3'; mouse calcineurin: 5' GCCGTTCCATTTCCACCAA 3'; mouse
13 NFATc3: 5' GGAGACATCAGTAGATGAT 3'; mouse MEF2C: 5' CCCACCTGGCAGCAAGAACAC
14 3'. The siRNA transduction was performed with lipofectamine 2000 (Invitrogen, cat#11668) according to
15 manufacturer's instruction. A final concentration of 50 nmol/L siRNA was used in the experiments. All
16 siRNAs were synthesized at RiboBio Co. Ltd. (Guangzhou, China).

18 **15. Statistical analysis**

19 Statistical analyses were performed using GraphPad Prism 6.0 for Windows (GraphPad Software,
20 San Diego, CA). All values were normally distributed (Kolmogorov-Smirnov test, $p > 0.10$ for each data
21 set). Student's t-test was performed for comparisons of two groups. One-way or two-way ANOVA (with
22 or without repeated measures) followed by Bonferroni's correction was performed for multiple group
23 comparisons. Data are given as mean \pm SEM, and a p-value of < 0.05 was considered significant. N
24 represents animal number, cell preparation rounds or independent culture experiments.

1 Supplemental References

- 2
- 3 1. Senyo SE, Steinhauser ML, Pizzimenti CL, Yang VK, Cai L, Wang M, Wu TD, Guerquin-Kern
4 JL, Lechene CP, Lee RT. Mammalian heart renewal by pre-existing cardiomyocytes. *Nature*.
5 2013;493:433-436.
- 6 2. Wang W, Zhang H, Gao H, Kubo H, Berretta RM, Chen X, Houser SR. β 1-adrenergic
7 receptor activation induces mouse cardiac myocyte death through both l-type calcium channel-
8 dependent and -independent pathways. *Am J Physiol Heart Circ Physiol*. 2010;299:H322-331.
- 9 3. Kubo H, Jaleel N, Kumarapeli A, Berretta RM, Bratinov G, Shan X, Wang H, Houser SR,
10 Margulies KB. Increased cardiac myocyte progenitors in failing human hearts. *Circulation*.
11 2008;118:649-657.
- 12 4. Takeda N, Manabe I, Uchino Y, Eguchi K, Matsumoto S, Nishimura S, Shindo T, Sano M, Otsu
13 K, Snider P, Conway SJ, Nagai R. Cardiac fibroblasts are essential for the adaptive response of
14 the murine heart to pressure overload. *J Clin Invest*. 2010;120:254-265.
- 15 5. Zaruba MM, Soonpaa M, Reuter S, Field LJ. Cardiomyogenic potential of c-kit(+)-expressing
16 cells derived from neonatal and adult mouse hearts. *Circulation*. 2010;121:1992-2000.
- 17 6. Chatterjee K, Zhang J, Honbo N, Simonis U, Shaw R, Karliner JS. Acute vincristine pretreatment
18 protects adult mouse cardiac myocytes from oxidative stress. *J Mol Cell Cardiol*. 2007;43:327-
19 336.
- 20 7. Remo BF, Qu J, Volpicelli FM, Giovannone S, Shin D, Lader J, Liu FY, Zhang J, Lent DS,
21 Morley GE, Fishman GI. Phosphatase-resistant gap junctions inhibit pathological remodeling and
22 prevent arrhythmias. *Circ Res*. 2011;108:1459-1466.
- 23 8. Turner MS, Haywood GA, Andreka P, You L, Martin PE, Evans WH, Webster KA, Bishopric
24 NH. Reversible connexin 43 dephosphorylation during hypoxia and reoxygenation is linked to
25 cellular atp levels. *Circ Res*. 2004;95:726-733.
- 26 9. Wang WE, Yang D, Li L, Wang W, Peng Y, Chen C, Chen P, Xia X, Wang H, Jiang J, Liao Q,
27 Li Y, Xie G, Huang H, Guo Y, Ye L, Duan DD, Chen X, Houser SR, Zeng C. Prolyl hydroxylase
28 domain protein 2 silencing enhances the survival and paracrine function of transplanted adipose-
29 derived stem cells in infarcted myocardium. *Circ Res*. 2013;113:288-300.
- 30 10. Suckau L, Fechner H, Chemaly E, Krohn S, Hadri L, Kockskamper J, Westermann D, Bisping E,
31 Ly H, Wang X, Kawase Y, Chen J, Liang L, Sipo I, Vetter R, Weger S, Kurreck J, Erdmann V,
32 Tschöpe C, Pieske B, Lebeche D, Schultheiss HP, Hajjar RJ, Poller WC. Long-term cardiac-
33 targeted rna interference for the treatment of heart failure restores cardiac function and reduces
34 pathological hypertrophy. *Circulation*. 2009;119:1241-1252.
- 35 11. Rui Y, Bai J, Perrimon N. Sarcomere formation occurs by the assembly of multiple latent protein
36 complexes. *PLoS Genet*. 2010;6:e1001208.

1 12. Eulalio A, Mano M, Dal Ferro M, Zentilin L, Sinagra G, Zacchigna S, Giacca M. Functional
2 screening identifies mirnas inducing cardiac regeneration. *Nature*. 2012;492:376-381.

3 13. Hsieh PC, Segers VF, Davis ME, MacGillivray C, Gannon J, Molkentin JD, Robbins J, Lee RT.
4 Evidence from a genetic fate-mapping study that stem cells refresh adult mammalian
5 cardiomyocytes after injury. *Nat Med*. 2007;13:970-974.

6 14. Tanaka M, Asada M, Higashi AY, Nakamura J, Oguchi A, Tomita M, Yamada S, Asada N,
7 Takase M, Okuda T, Kawachi H, Economides AN, Robertson E, Takahashi S, Sakurai T,
8 Goldschmeding R, Muso E, Fukatsu A, Kita T, Yanagita M. Loss of the bmp antagonist usag-1
9 ameliorates disease in a mouse model of the progressive hereditary kidney disease alport
10 syndrome. *J Clin Invest*. 2010;120:768-777.

11 15. Xin M, Kim Y, Sutherland LB, Murakami M, Qi X, McAnally J, Porrello ER, Mahmoud AI, Tan
12 W, Shelton JM, Richardson JA, Sadek HA, Bassel-Duby R, Olson EN. Hippo pathway effector
13 yap promotes cardiac regeneration. *Proc Natl Acad Sci U S A*. 2013;110:13839-13844.

14
15
16
17
18
19
20
21
22
23
24
25
26
27
28
29
30
31
32
33
34
35
36

1 **Supplemental Figure Legends**

2
3 **Supplemental Figure 1:** ACM survival in *in-vitro*. **A:** Representative images of ACMs isolated from β -
4 actin-GFP mice cultured in control medium. Trypan blue staining was used to identify ACM death. GFP
5 positive/trypan blue negative cells were counted as live cells. **B:** Representative images of ACMs co-
6 cultured with NRVM. **C:** Survival rate of ACMs co-cultured with NRVMs, co-cultured with fibroblasts,
7 in conditioned medium of NRVMs (transwell system) and in normal medium. Scale bars represent 50 μ m.
8 N=6, * $p < 0.05$ vs. control; # $p < 0.05$ vs. transwell at the same time points.

9
10 **Supplemental Figure 2:** The proliferation of genetic fate-mapping ACMs and the Ca^{2+} transmission from
11 NRVMs to ACMs. **A:** Structure of Myh6-MerCreMer-tdTomato allele. B6.FVB(129)-Tg(Myh6-
12 cre/Esr1)1Jmk/J mice were crossbred with B6.Cg-Gt(ROSA)26Sortm14(CAG-tdTomato)Hze/J. **B:** The
13 morphological remodeling and proliferation of a representative ACM isolated from Myh6-MerCreMer-
14 tdTomato mouse co-culture with NRVMs, observed with a time-lapse video microscopy. The
15 proliferation process of this ACM can be found in **Supplemental Video 5**.

16
17 **Supplemental Figure 3:** Exclusion of cell fusion in the ACM-DPR process. **A:** NRVMs were infected
18 with adenoviral RFP, and then co-cultured with GFP positive pre-existing ACMs from β -actin-GFP
19 transgenic mice. Approximately 8,500 GFP⁺ cells were counted, and no cell with co-expression of GFP
20 and RFP was detected at day 7 post-coculture. **B:** ACMs isolated from Myh6-MHC-MerCreMer-
21 tdTomato mice were mixed with cardiac non-myocytes isolated from β -actin-GFP mice, which were then
22 co-cultured with NRVMs. More than 15,000 tdTomato⁺ cells from three mice were counted, and 4 cells
23 with co-expression of tdTomato and GFP were detected at day 7 post-coculture. **B1:** Representative
24 images of a tdTomato⁺ cell without GFP expression. **B2:** Representative images of a tdTomato⁺/GFP⁺ cell.
25 Scale bars represent 20 μ m.

26
27 **Supplemental Figure 4:** Direct co-culture with contracting cardiomyocytes induces ACM
28 redifferentiation. **A:** Representative images of ACM morphological change in co-culture and in a
29 transwell system at 7 days post-culture with NRVMs. **B:** Representative images (B1) and percentage
30 quantification (B2) of ACMs with sarcomere reappearance co-cultured with NRVMs, FCMs or
31 fibroblasts at day 7. **C:** The percentage of spontaneous beating ACMs in different co-culture systems at
32 day 7. **D:** The proliferation rate with complete cytokinesis of ACMs co-cultured with NRVMs or non-
33 myocytes, observed by a time-lapse imaging system. **E:** The % of ACMs daughter cells with sarcomere
34 re-organization, in the co-culture with NRVMs or non-myocytes, N=6. * $p < 0.05$ vs. Fibroblast or non-
35 myocytes. Scale bars represent 50 μ m.

1 **Supplemental Figure 5:** The specific knockdown of Cx43 in ACMs by mouse specific Cx43-siRNA. **A:**
2 The representative images of fluorescence recovery after photo bleaching (FRAP) to assess gap junction
3 connections between ACMs and NRVMs. Cell-permeant dye calcein red-orange AM was used for FRAP
4 analysis. **B:** The Ca^{2+} transient propagation from spontaneously beating NRVMs to neighboring ACMs.
5 **B1:** A representative image of cytoplasmic free Ca^{2+} labeling with Fluo-4 AM in the co-culture of ACMs
6 and NRVMs. White line in the cell image indicates the scan line crossing an ACM and its neighboring
7 NRVM. **B2:** Line-scan image analysis of Ca^{2+} transient transmission from spontaneously beating NRVMs
8 to neighboring ACM. For B1-2, red fluorescence indicates the fate-mapping Myh6-MerCreMer-tdTomato
9 ACM and green fluorescence indicates the fluo-4 labeled cytoplasmic free Ca^{2+} . The Ca^{2+} waves of this
10 co-coculture can be found **Supplemental Video 6.** **C:** The mouse specific mRNA expression of Cx43
11 analyzed with qPCR. N=7, * $p < 0.05$ vs. scramble. **D:** Immunostaining against Cx43 in the co-culture. In
12 co-culture pretreated with scramble siRNA, arrow “a” indicates an ACM that expressing Cx43, while
13 arrow “b” indicates neighboring NRVMs expressing Cx43. In co-culture pretreated with Cx43-siRNA,
14 arrow “c” indicates an ACM with little Cx43 expression, while arrow “d” indicates neighboring NRVMs
15 expressing Cx43. For A-D, scale bars represent $30\mu\text{m}$.

16
17 **Supplemental Figure 6:** Strategy for genetic fate-mapping of adult Myh6-MerCreMer-lacZ mouse
18 cardiomyocytes and their progeny in mice. **A:** Structure of Myh6-MerCreMer-lacZ allele. B6.FVB (129)-
19 Tg(Myh6-cre/Esr1)1Jmk/J mice were crossbred with B6.129S4-Gt(ROSA)26Sortm1Sor/J mice. **B:**
20 Representative images of pre-existing ACMs with X-gal (lacZ staining). Labeling efficiency of the mouse
21 line was $> 90\%$. Scale bars represent $50\mu\text{m}$.

22
23 **Supplemental Figure 7:** ACMs with proliferation marker EdU express fate-mapping marker lacZ in
24 post-MI hearts. Tamoxifen injected Myh6-MerCreMer-lacZ mice were suffered from MI injury, followed
25 by EdU incorporation analysis. Immunotaining on both heart tissue and isolated heart cells were then
26 performed. **A:** Representative images of lacZ immunostaining of infarcted area 3 weeks post-MI. LacZ
27 staining tracks pre-existing cardiomyocytes. Arrow “a” indicates infarcted area while arrow “b” indicates
28 survived myocardium. Scale bars represent $50\mu\text{m}$. **B:** Representative images of a
29 $\text{lacZ}^+/\text{EdU}^+/\text{tropomyosin}^+$ ACM in infarct border zone 3 weeks post-MI. **C:** Representative images of both
30 mononuclear and binuclear $\text{lacZ}^+/\text{EdU}^+/\text{tropomyosin}^+$ ACMs isolated from hearts 3 weeks post-MI. For
31 B-C, scale bars represent $20\mu\text{m}$.

32
33 **Supplemental Figure 8:** The redifferentiation of ACMs in post-MI hearts with different treatments. The
34 post-MI hearts were treated with AAV-9-Cx43-S3E, Cx43-siRNA or CsA, respectively. EdU
35 incorporation was performed and the immunostaining was conducted on the isolated ACMs 2 weeks post-
36 MI. **A:** Representative images of $\text{EdU}^+/\text{tropomyosin}^+$ cardiomyocytes with or without re-organized
37 sarcomere. **B1:** The total number of $\text{EdU}^+/\text{tropomyosin}^+$ cardiomyocytes in post-MI hearts. B2: The
38 proportion of sarcomere $^+$ cardiomyocytes out of the total $\text{EdU}^+/\text{tropomyosin}^+$ cardiomyocyte in post-MI
39 hearts. N=7; * $p < 0.05$ vs. AAV-vector; # $p < 0.05$ vs. Scramble; & $p < 0.05$ vs. DMSO.

1
2
3
4
5
6
7
8
9
10
11
12
13
14
15
16
17
18
19
20
21
22
23
24
25
26
27
28
29
30
31
32
33
34
35
36
37
38
39
40

Supplemental Figure 9: The distribution of newly formed cardiomyocytes in post-MI heart. EdU incorporation analysis and tropomyosin staining were used to detect newly formed cardiomyocytes 3 weeks post-MI. **A:** Representative images of the distribution of EdU⁺/tropomyosin⁺ cells in remote area and infarct border zone. Arrows indicate EdU⁺/tropomyosin⁺ cells, which were presumed as new cardiomyocytes. **B:** Quantification of EdU⁺/tropomyosin⁺ cells in remote area and infarct border zone. N=8, * p<0.05 vs. remote area. Scale bars represent 50µm.

Supplemental Figure 10: A schematic diagram for the process of mouse ACM dedifferentiation, proliferation and redifferentiation. Ischemia induces ACM dedifferentiation, accompanied with gap junction dysfunction and ACM uncoupling. Dedifferentiated ACM can proliferate and redifferentiate. ACM redifferentiation requires Cx43 mediated re-coupling to a neighboring myocyte with Ca²⁺ transients. Calcineurin-NFAT signaling pathway was involved in the Ca²⁺ mediated ACM redifferentiation. Stabilization of Cx43 phosphorylation against ischemia helps the process of ACM proliferation and redifferentiation.

1 **Legends for the Video Files**

2

3 **Supplemental Video 1:** Proliferation (with completed cytokinesis) of a bi-nucleated ACM isolated from
4 transgenic β -actin-GFP mouse co-cultured with NRVMs, recorded by live cell imaging using time-lapse
5 microscopy. ACMs were pretreated with Thermo Scientific DRAQ5™ Fluorescent Probe to label nuclei
6 (red fluorescence) before co-culture with NRVMs. The time-lapse images were taken at intervals of one
7 hour for 7 days. Representative frames of this video at different time points can be found in **Figure 2A**.

8

9 **Supplemental Videos 2-4:** Representative proliferating ACM examples with completed cytokinesis
10 captured by live cell imaging using time-lapse microscopy. Green fluorescence represents ACMs isolated
11 from adult β -actin-GFP transgenic mouse. The nuclei of ACMs were labeled with red fluorescence by
12 Thermo Scientific DRAQ5™ Fluorescent Probe. The progeny of these proliferated ACMs were
13 immunostained after the 7-days-co-culture, and the results were presented in **Figure 2E**.

14

15 **Supplemental Videos 5:** Proliferation (with completed cytokinesis) of a bi-nucleated ACM isolated from
16 fate-mapping Myh6-MerCreMer-tdTomato mouse co-cultured with NRVMs, recorded by live cell
17 imaging using time-lapse microscopy. The time-lapse images were taken at intervals of one hour for 7
18 days. Representative frames of this video at different time points can be found in **Supplemental Figure**
19 **3B**.

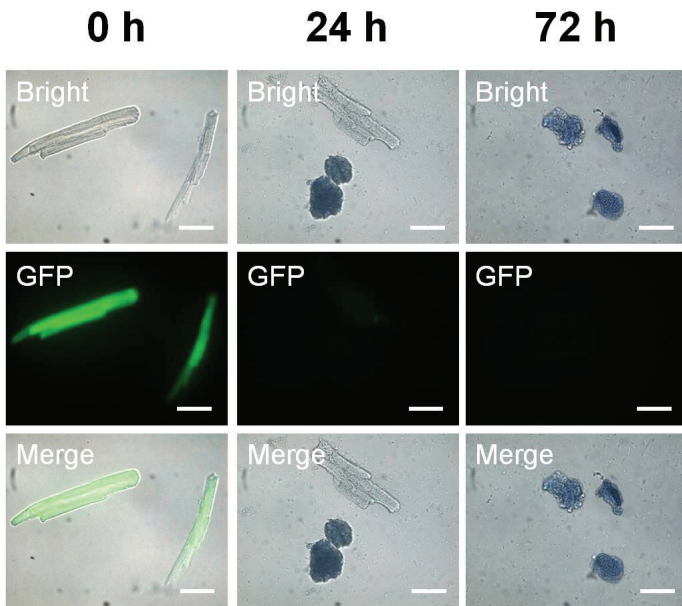
20

21 **Supplemental Videos 6:** The Ca^{2+} transient propagation from spontaneously beating NRVMs to
22 neighboring ACMs. Red fluorescence indicates the fate-mapping Myh6-MerCreMer-tdTomato ACM and
23 green fluorescence indicates the fluo-4 labeled cytoplasmic free Ca^{2+} . Line-scan image analysis of these
24 coupled cells was shown in **Supplemental Figure 3B**.

Supplemental Figure 1

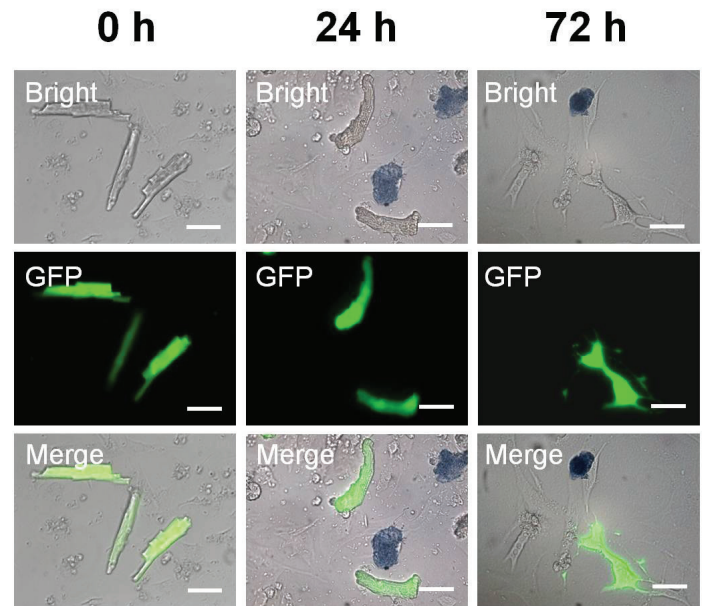
A

ACMs in control medium

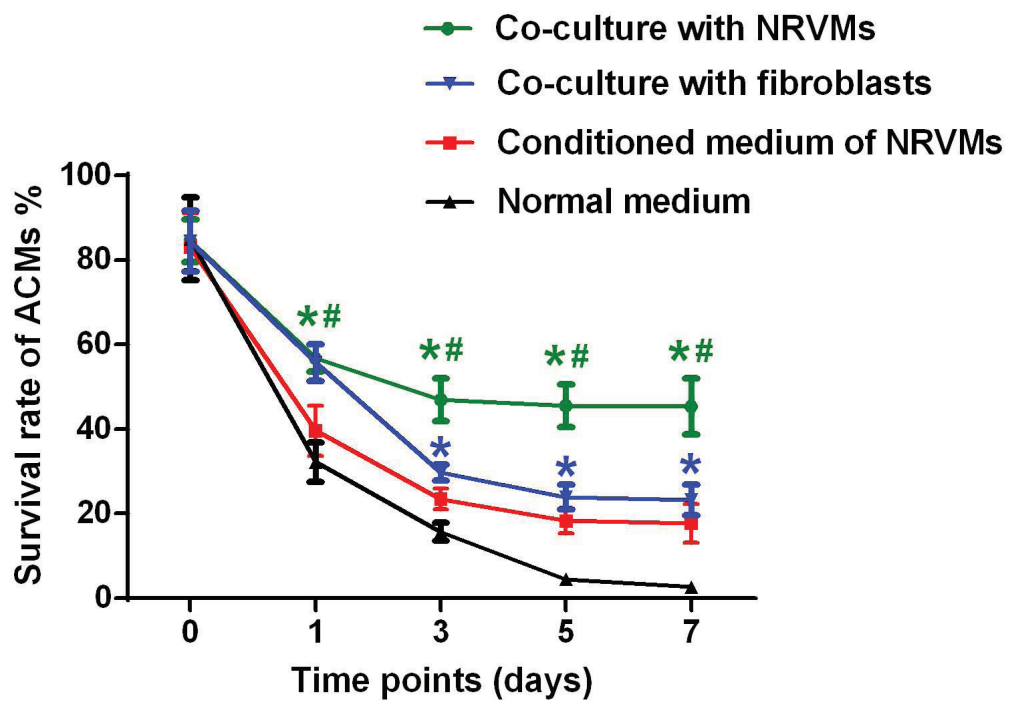


B

ACMs co-cultured with NRVMs

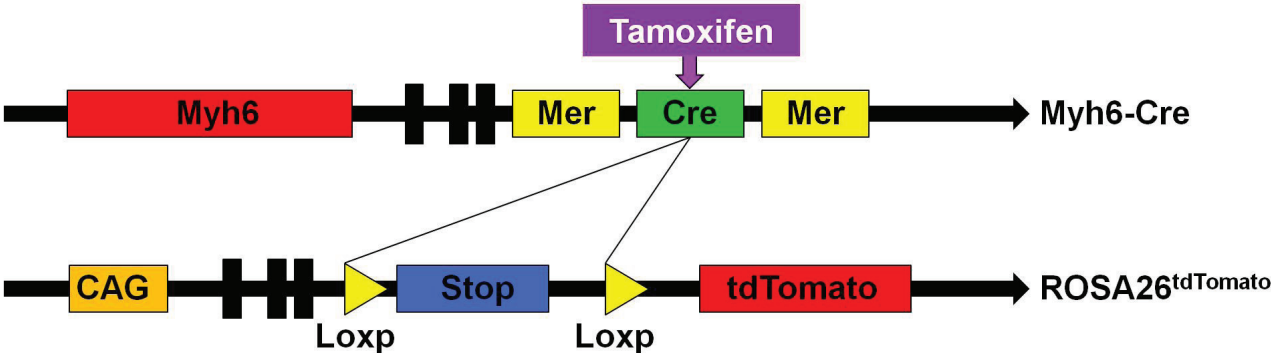


C

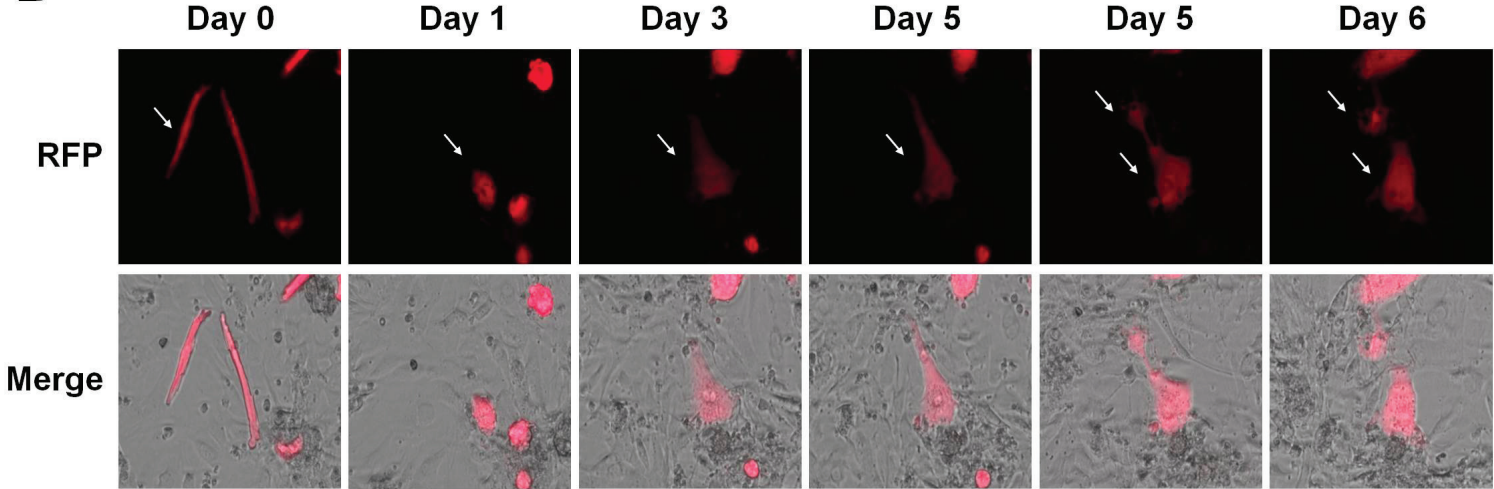


Supplemental Figure 2

A

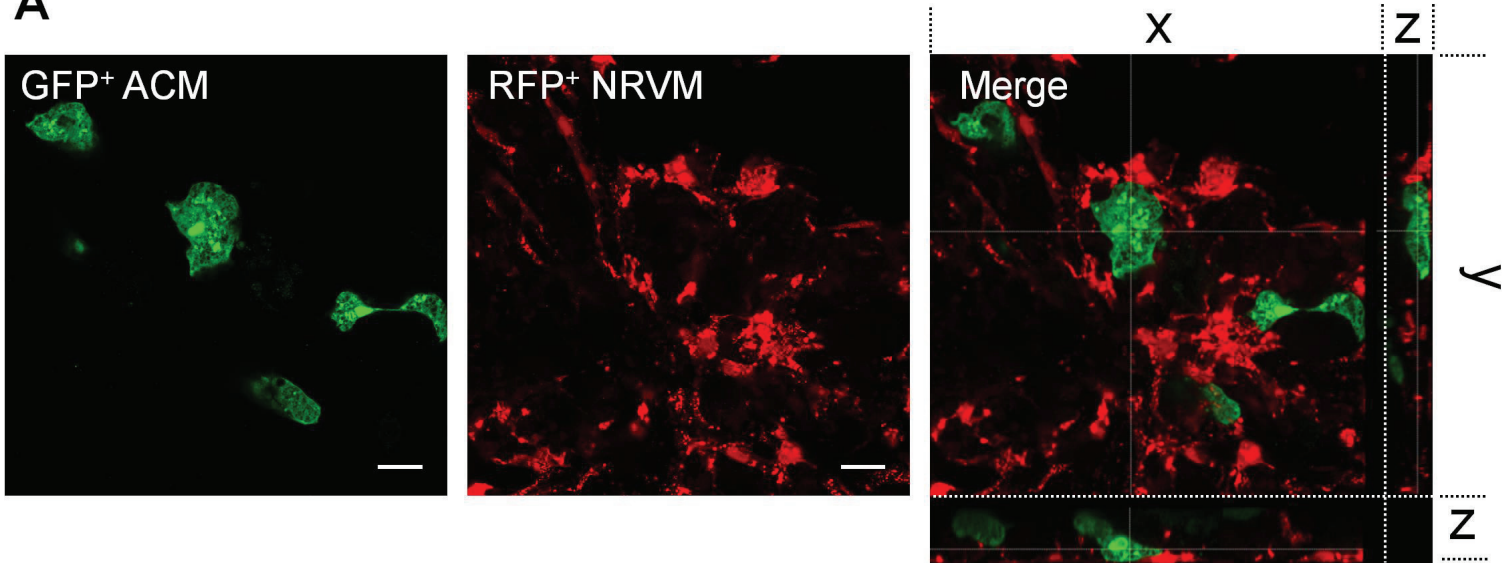


B

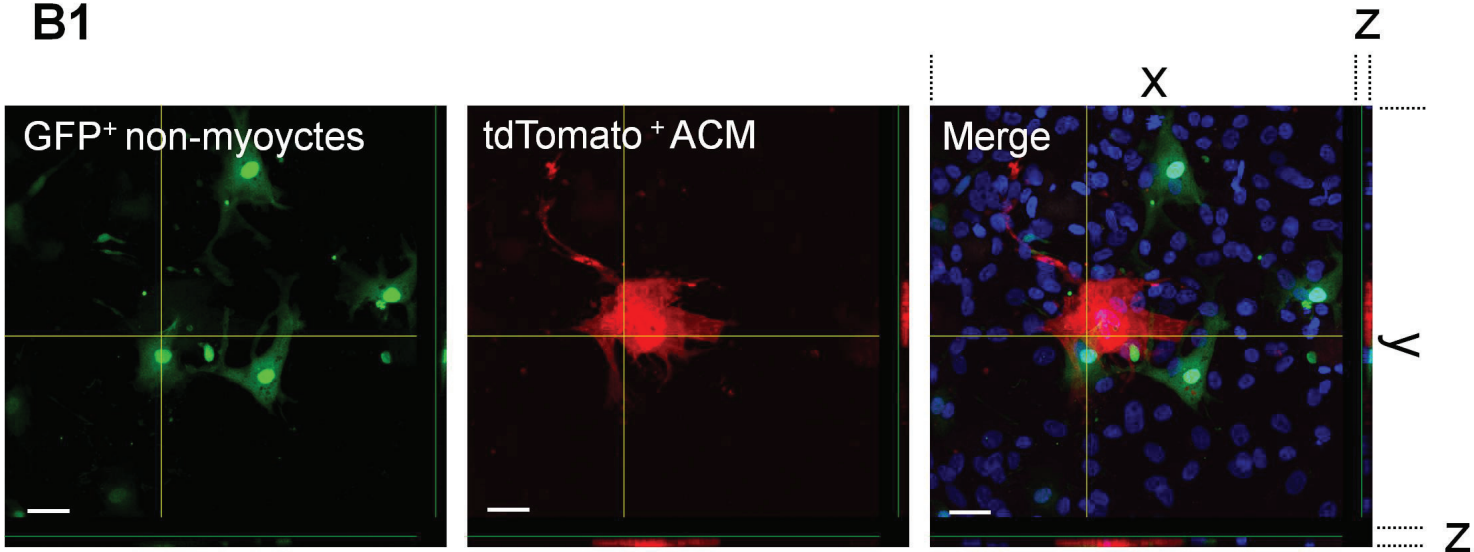


Supplemental Figure 3

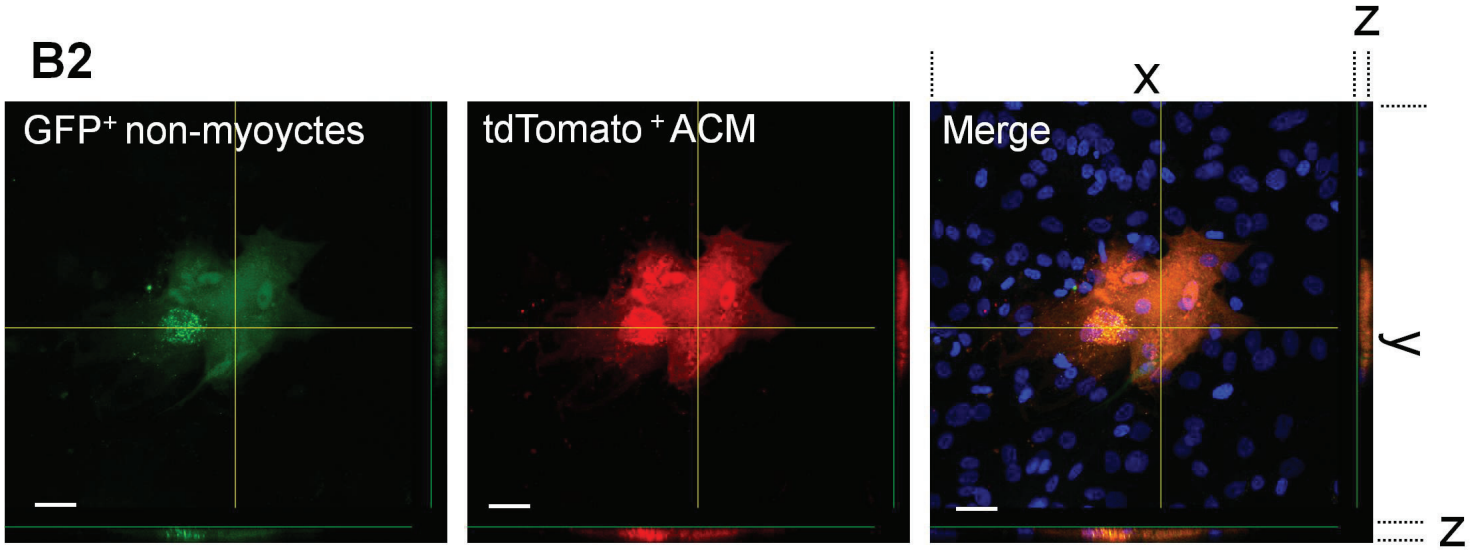
A



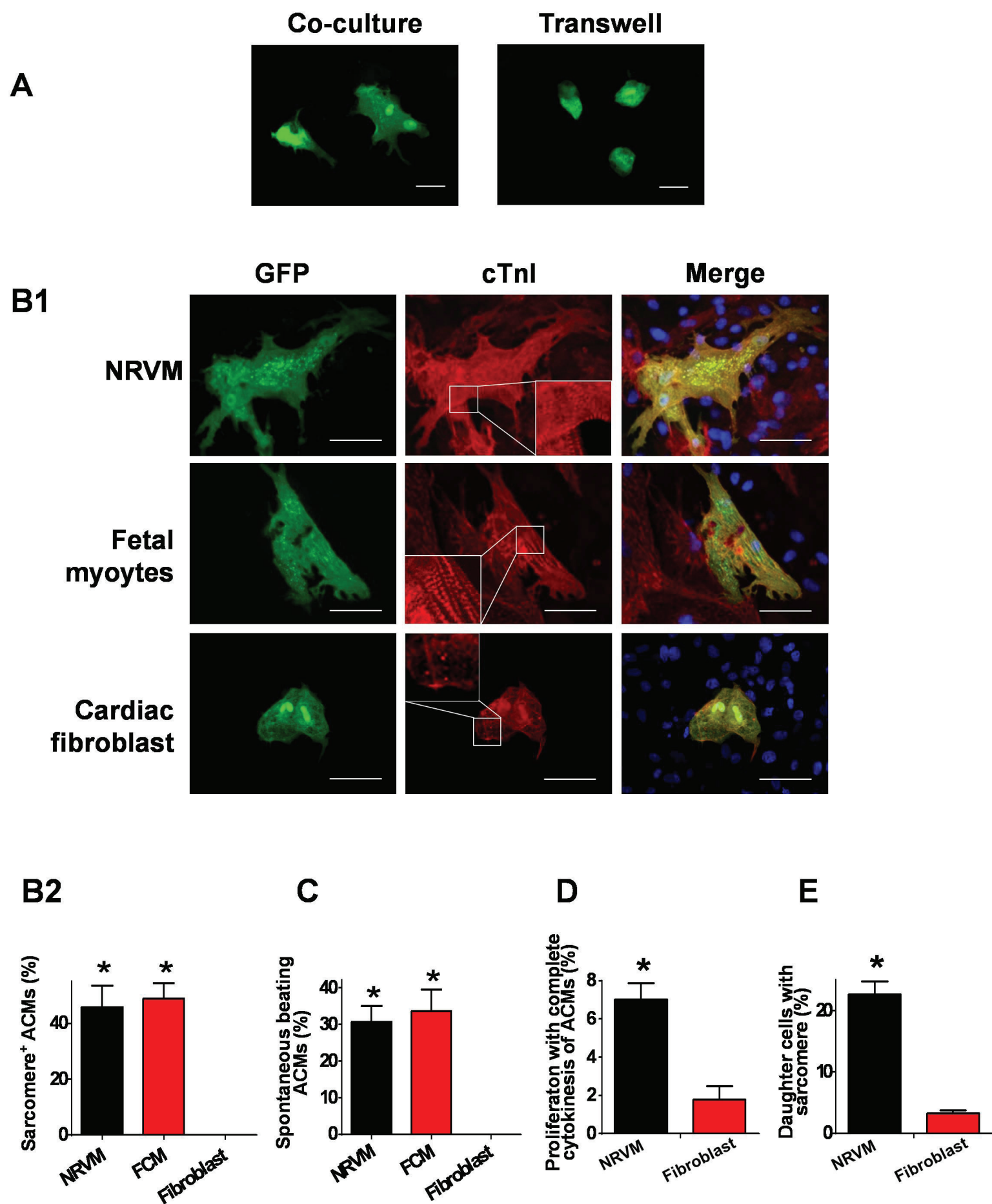
B1



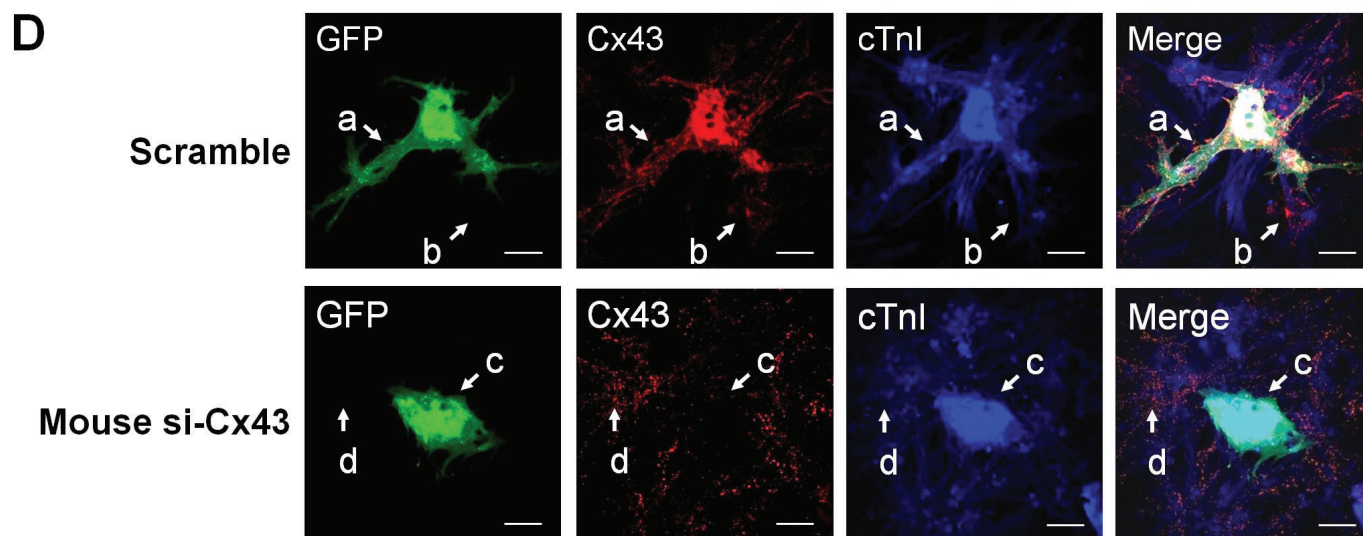
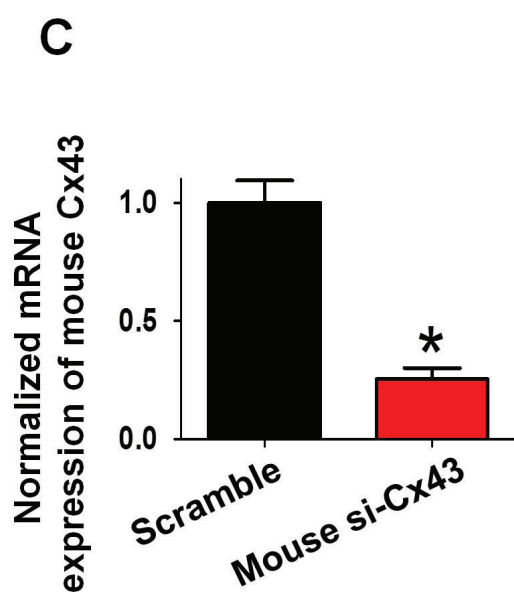
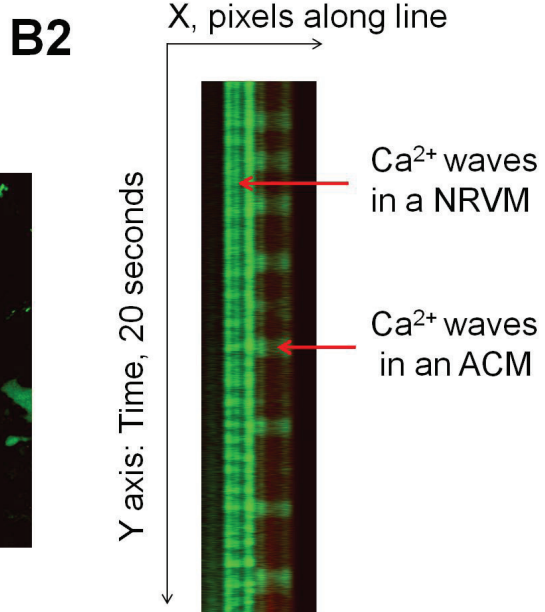
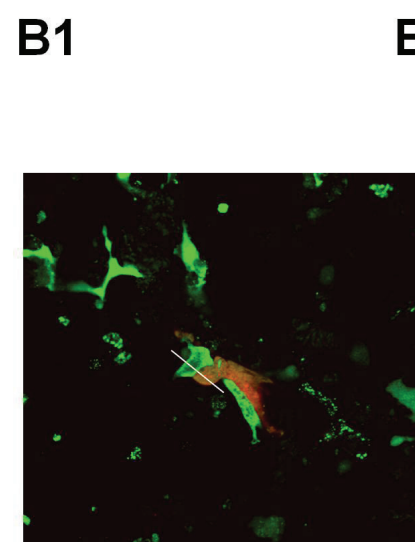
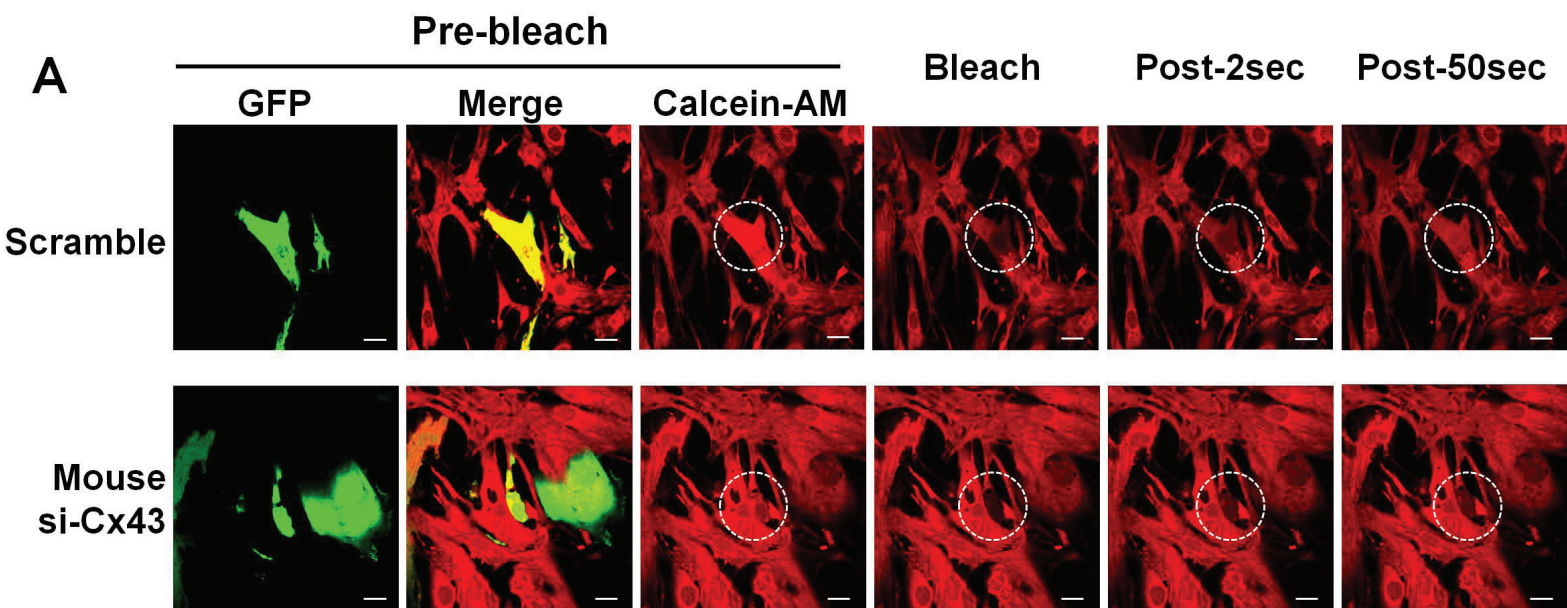
B2



Supplemental Figure 4

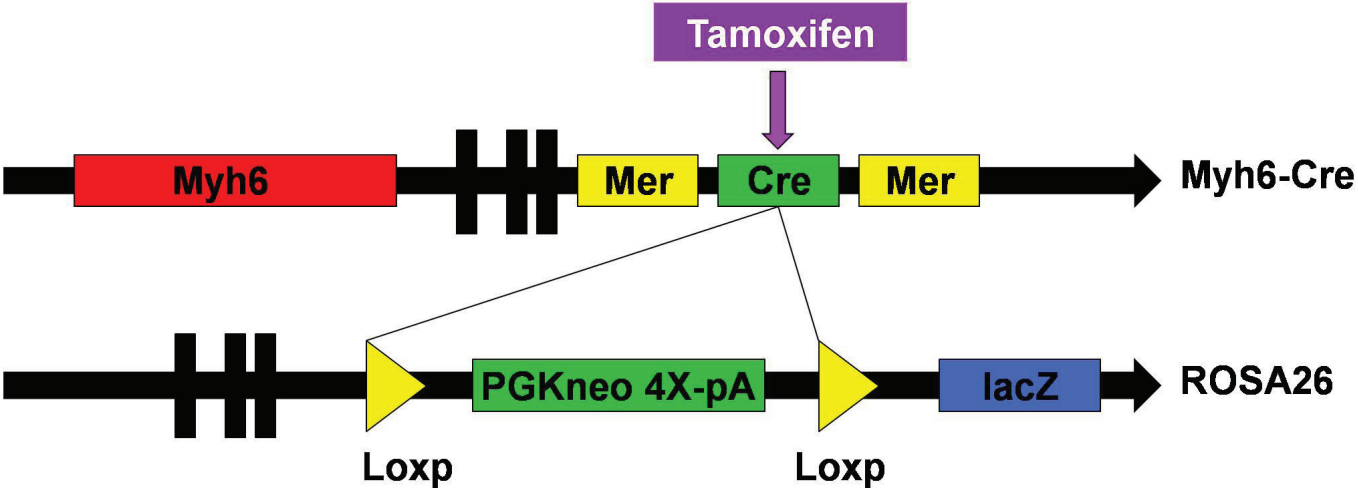


Supplemental Figure 5



Supplemental Figure 6

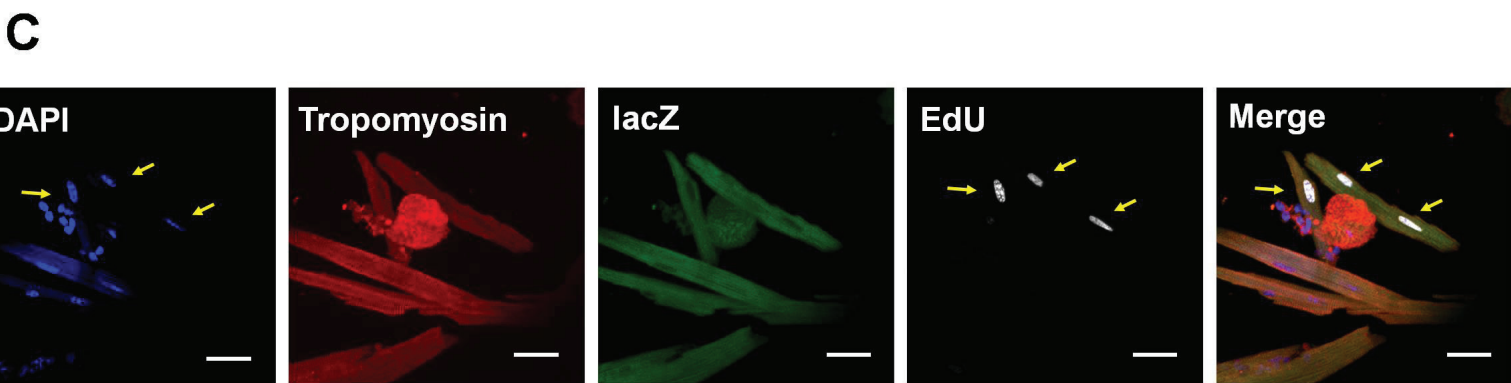
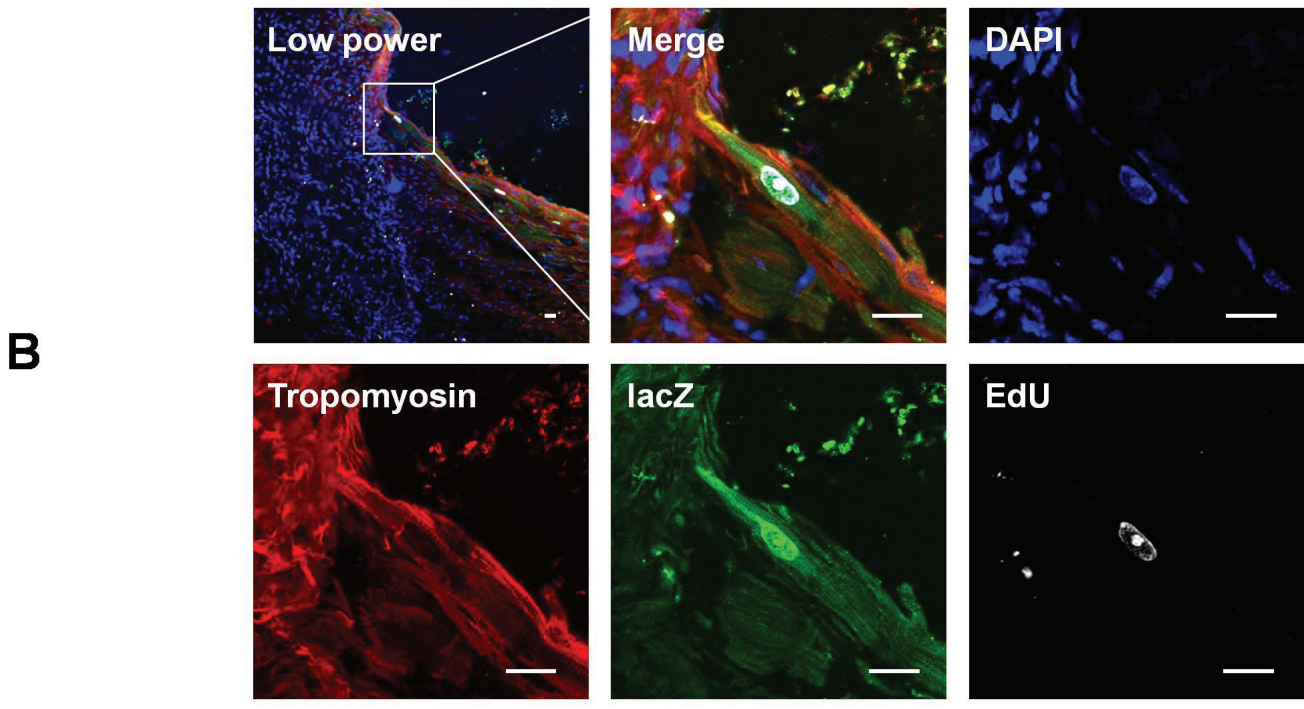
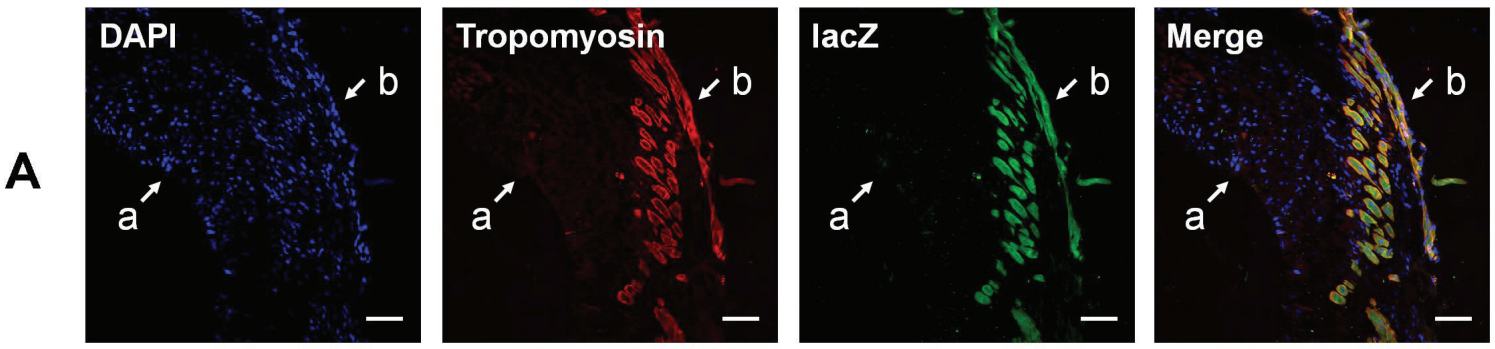
A



B

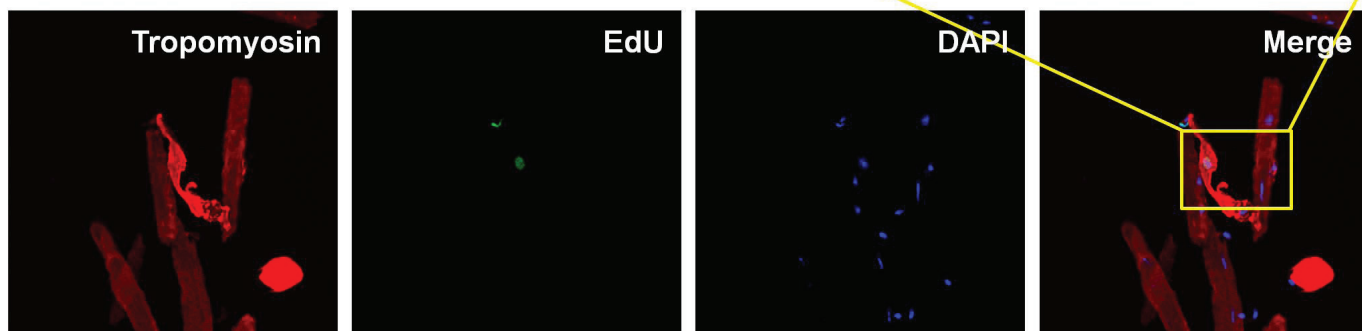


Supplemental Figure 7

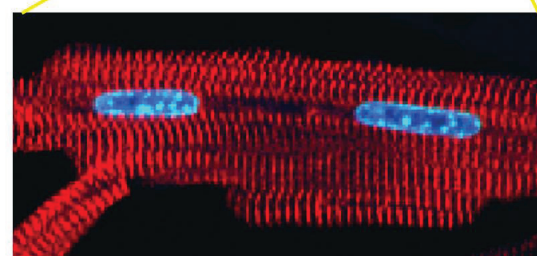
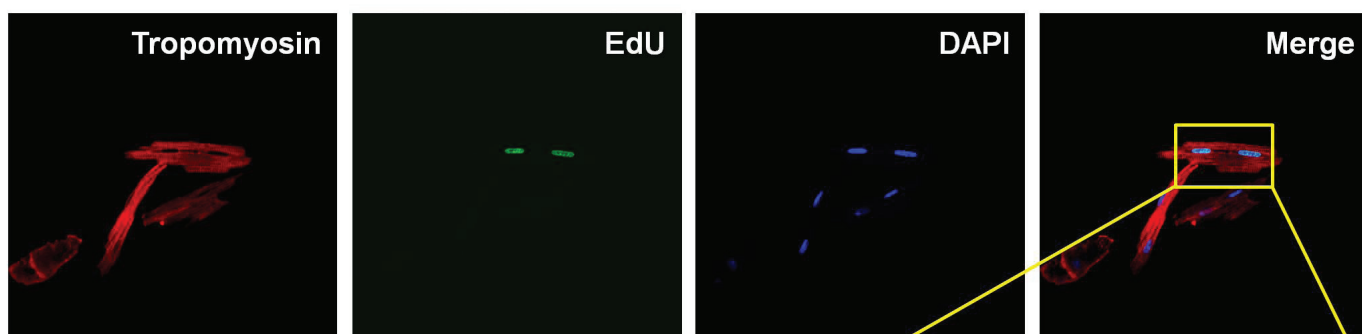


Supplemental Figure 8

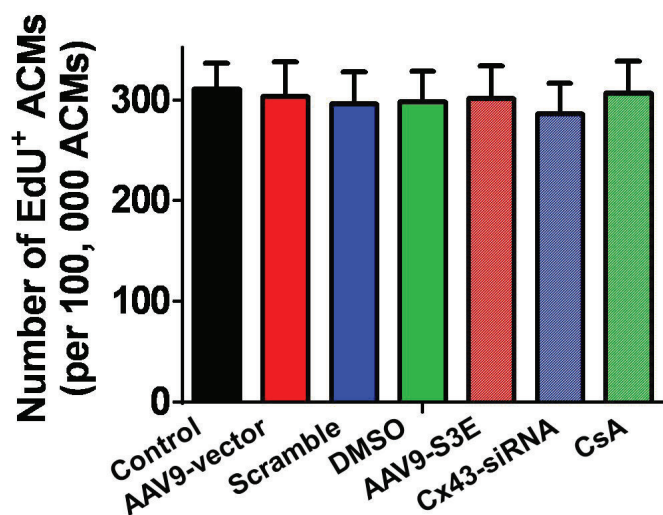
A1



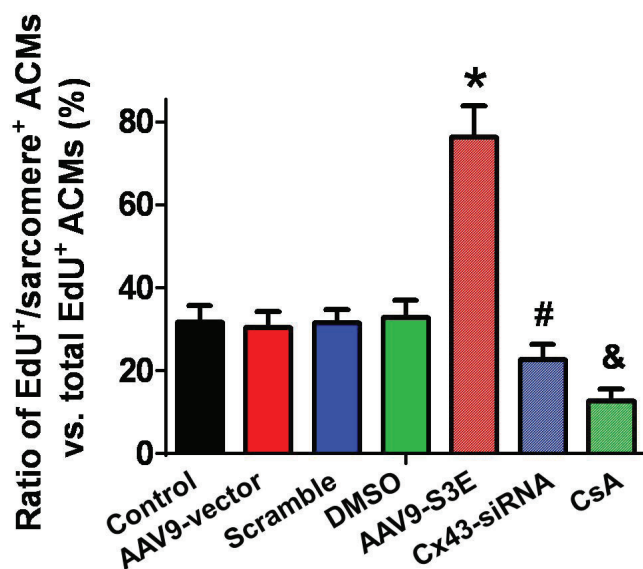
A2



B1

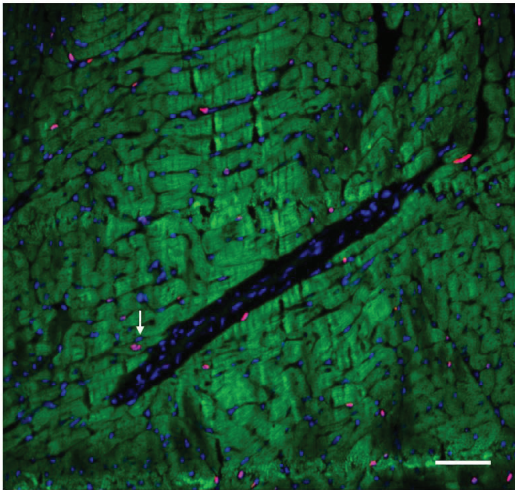


B2

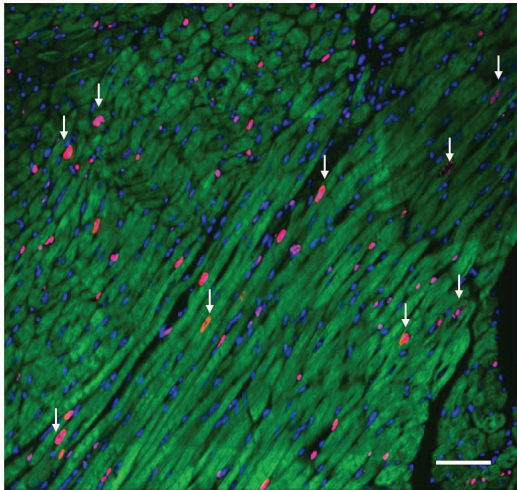


Supplemental Figure 9

A

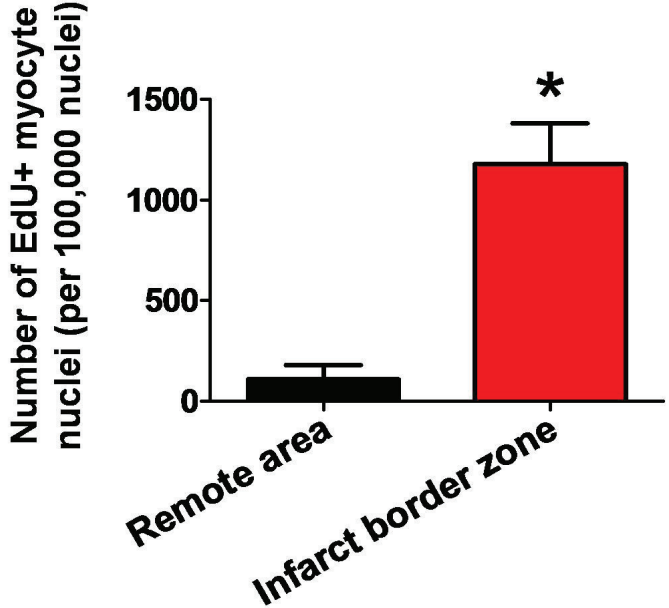


Remote area



Infarct border zone

B



Supplemental Figure 10

